Mathematics

http://www.aimspress.com/journal/Math

AIMS Mathematics, 8(10): 24446–24472.
DOI: 10.3934/math.20231247
Received: 12 June 2023
Revised: 23 July 2023
Accepted: 09 August 2023
Published: 17 August 2023

Research article

Dynamic complexity of a slow-fast predator-prey model with herd behavior

Ahmad Suleman[1,†], Rizwan Ahmed[1], Fehaid Salem Alshammari[2,*] and Nehad Ali Shah[3,†]

[1] Department of Mathematics, Air University Multan Campus, Multan, Pakistan

[2] Department of Mathematics and Statistics, Faculty of Science, Imam Mohammad Ibn Saud Islamic University (IMSIU), Riyadh, Saudi Arabia

[3] Department of Mechanical Engineering, Sejong University, Seoul 05006, South Korea

* **Correspondence:** Email: falshammari@imamu.edu.sa.

[†] These authors contributed equally to this work and are co-first authors.

Abstract: The complex dynamics of a slow-fast predator-prey interaction with herd behavior are examined in this work. We investigate the presence and stability of fixed points. By employing the bifurcation theory, it is shown that the model undergoes both a period-doubling and a Neimark-Sacker bifurcation at the interior fixed point. Under the influence of period-doubling and Neimark-Sacker bifurcations, chaos is controlled using the hybrid control approach. Moreover, numerical simulations are carried out to highlight the model's complexity and show how well they agree with analytical findings. Employing the slow-fast factor as the bifurcation parameter shows that the model goes through a Neimark-Sacker bifurcation for greater values of the slow-fast factor at the interior fixed point. This makes sense because if the slow-fast factor is large, the growth rates of the predator and its prey will be about identical, automatically causing the interior fixed point to become unstable owing to the predator's slow growth.

Keywords: slow-fast; predator-prey; square root functional response; stability; bifurcation; hybrid control
Mathematics Subject Classification: 39A28, 39A30

1. Introduction

Differential equations are crucial in understanding and explaining the dynamic behavior of complex systems in a variety of scientific areas. Differential equations are extensively used in ecology to simulate population dynamics, predator-prey interactions and the interactions between species in ecosystems [1, 2]. Differential equations are used in economics to simulate economic development, investment and consumption patterns [3, 4]. The Navier-Stokes equations regulate fluid motion in fluid mechanics, allowing the study of fluid flow patterns, turbulence and the behavior of gases and liquids [5–7]. Differential equations are used in a variety of domains, including engineering, epidemiology, neurology and climate research. In mathematical ecology, studying the dynamics between predators and prey is one of the most significant research subjects. It is also one of the most fundamental interspecies relationships in ecology and the foundation of the complex food chain. The Lotka-Volterra models are the most well-known predator-prey models. These models are polynomial differential equations of degree two, initially proposed by Alfred J. Lotka [8] and Vito Volterra [9]. Since then, several researchers have made developments while considering a wide range of biological phenomena.

We consider a Gauss-type predator-prey interaction when the prey exhibits group defense, which is represented by the following set of ordinary differential equations [10]:

$$\begin{cases} \frac{dx}{dt} = rx(1 - \frac{x}{k}) - p(x)y, \\ \frac{dy}{dt} = -dy + cp(x)y, \end{cases} \tag{1.1}$$

where x, y, r, k, d and c are the population density of prey, the population density of predator, the growth rate of prey, the prey's carrying capacity, the predator's death rate and the efficiency of the predator in converting the consumed prey into the predator's offspring, respectively. The functional response $p(x)$ represents the instantaneous rate of prey depletion per predation.

In population dynamics, the functional response is an important feature of all predator-prey interactions. It illustrates the link between the predator's consumption rate and the density of prey. It represents the quantity of prey that is ingested by individual predators. Holling [11] proposed three distinct forms of functional responses in 1965. After that, researchers like Crowley-Martin [12] and Beddington-DeAngelis [13, 14] proposed different functional responses. Later, other researchers investigated predator-prey interactions, including various kinds of functional responses [15–21].

Some prey populations display herd behavior, meaning predator-prey interaction happens along the prey population's boundaries. The Holling-type functional response cannot adequately describe this form of interaction. In fact, a class of prey population shows herd behavior. Hence, a predator's rate of prey capture differs from standard models. For instance, a fish's capture rate of zooplankton in the ocean is greater than its capture rate of phytoplankton. Phytoplankton exhibits herding behavior in this environment.

Ajraldi et al. [22] investigated the following model:

$$\begin{cases} \frac{dR(t)}{dt} = rR(t)(1 - \frac{R(t)}{k}) - a\sqrt{R(t)}F(t), \\ \frac{dF(t)}{dt} = -\tilde{m}F(t) + a\tilde{e}\sqrt{R(t)}F(t). \end{cases} \tag{1.2}$$

They considered the prey population's square root to examine the prey population's herd behavior such that the predator interacts with the prey throughout the herd's outer corridor. It has been shown that the sustained limit cycles are possible and the solution behavior near the origin is more subtle and interesting than the classical predator-prey models. The square root functional response predator-prey model has been investigated and discussed by several scientists [23–26]. After incorporating the square root functional response, the model (1.1) transforms to:

$$\begin{cases} \frac{dx}{dt} = rx(1 - \frac{x}{k}) - a\sqrt{x}y, \\ \frac{dy}{dt} = -dy + b\sqrt{x}y, \end{cases} \tag{1.3}$$

where a represents the predator's search efficiency and $b = ac$.

According to the species' traits, the prey population often increases considerably more quickly than the predator's; hares and lynx are well-known examples where hares reproduce much more rapidly than lynx [27]. This inspired the researchers to add a small time-scale parameter $0 < \epsilon < 1$ to the fundamental model. The parameter ϵ may be interpreted as the ratio between the predator's linear mortality rate and the prey's linear growth rate [28, 29]. The assumption that $\epsilon < 1$ means that one generation of predators may come into contact with several generations of prey. As a result, the following may be written for the slow-fast version of the model (1.3):

$$\begin{cases} \frac{dx}{dt} = rx(1 - \frac{x}{k}) - a\sqrt{x}y, \\ \frac{dy}{dt} = \epsilon(-dy + b\sqrt{x}y). \end{cases} \tag{1.4}$$

Due to the square root term, the Jacobian of the above model (1.4) possesses a singularity. We utilize the transformations $x(t) = u^2(t)$ and $y(t) = v(t)$ to understand it better. After applying the transformation, the system (1.4) transforms to

$$\begin{cases} \frac{du}{dt} = \frac{ru}{2}(1 - \frac{u^2}{k}) - \frac{av}{2}, \\ \frac{dv}{dt} = \epsilon(-dv + buv). \end{cases} \tag{1.5}$$

It is worth noting that many biological models are governed by continuous and discrete models. Several researchers have made significant contributions to discrete models in recent years [30–33]. This is due to the fact that discrete models are considerably more effective than continuous models at nonoverlapping generations. It has been demonstrated that discrete-time models have the benefit of making it easier to acquire numerical solutions. In addition, substantial research has shown that discrete-time models display more complicated dynamical behaviors than continuous-time models [34–39]. So, our primary motivation in this study is to consider the discrete-time counterpart of the predator-prey model (1.5). The model to be analyzed in this work is then obtained using the forward Euler technique on the model (1.5) as follows:

$$\begin{cases} u_{n+1} = u_n + \frac{h}{2}\Big(ru_n(1 - \frac{u_n^2}{k}) - av_n\Big), \\ v_{n+1} = v_n + \epsilon h v_n(-d + bu_n), \end{cases} \tag{1.6}$$

where h is the step size.

The present investigation's primary findings and deductions are as follows:

- We investigate the presence and topological categorization of fixed points.
- The results of our study indicate that the mathematical system represented by Eq (1.6) undergoes both period-doubling (PD) and Neimark-Sacker (NS) bifurcations.
- The present study investigates the conditions for the existence and direction of NS and PD bifurcation at the positive fixed point.
- In order to rein in the unpredictability of the system (1.6), a hybrid approach to control is used.

We suggest readers to [40–43] for some interesting studies on the investigation of stability, bifurcation and chaos control over predator-prey interactions. The remainder of the paper is structured as follows:

In Section 2, we first examine the existence and stability of fixed points. Then, in Section 3, we demonstrate how, under appropriate conditions for parameter values, the model (1.6) may experience PD and NS bifurcation. In Section 4, we study a hybrid control strategy for dealing with chaos. In Section 5, numerical simulations illustrate the viability of the key theoretical findings. Section 6 contains conclusions based on our findings.

2. Fixed points' existence and topological classification

We solve the following system of equations to obtain the fixed points $(\bar{u}, \bar{v})$ of the model (1.6):

$$\begin{cases} \bar{u} = \bar{u} + \frac{h}{2}\Big(r\bar{u}(1 - \frac{(\bar{u})^2}{k}) - a\bar{v}\Big), \\ \bar{v} = \bar{v} + \epsilon h\bar{v}(-d + b\bar{u}). \end{cases} \tag{2.1}$$

The three fixed points obtained are as follows:

$$E_0 = (0, 0), \; E_1 = (\sqrt{k}, 0), E_2 = \left(\frac{d}{b}, \frac{d(-d^2 + b^2k)r}{ab^3k}\right).$$

E_0, E_1 are boundary fixed points. The model (1.6) possesses a unique interior fixed point, E_2, exclusively when the carrying capacity of prey satisfies the condition $k > \frac{d^2}{b^2}$.

The Jacobian matrix J of the model (1.6) computed at fixed point $(\bar{u}, \bar{v})$ is provided by

$$J(\bar{u}, \bar{v}) = \begin{bmatrix} 1 + \frac{rh(k-3(\bar{u})^2)}{2k} & -\frac{ah}{2} \\ bh\epsilon\bar{v} & 1 - dh\epsilon + bh\epsilon\bar{u} \end{bmatrix}.$$

We use the following two results for topological classification of the fixed points of the model (1.6):

Lemma 2.1. *[44] Let $\Upsilon(\xi) = \xi^2 + A_1\xi + A_0$ be the characteristic polynomial of $J(\bar{x}, \bar{y})$ and $\xi_{1,2}$ satisfy $\Upsilon(\xi) = 0$, then the fixed point $(\bar{x}, \bar{y})$ is a*

(1) sink (locally asymptotically stable (LAS)) if $|\xi_{1,2}| < 1$,

(2) source if $|\xi_{1,2}| > 1$,

(3) saddle point (SP) if $|\xi_1| < 1$ and $|\xi_2| > 1$ (or $|\xi_1| > 1$ and $|\xi_2| < 1$),

(4) non-hyperbolic point (NHP) if either $|\xi_1| = 1$ or $|\xi_2| = 1$.

Lemma 2.2. *[44] Let $\Upsilon(\xi) = \xi^2 + A_1\xi + A_0$. Assume that $\Upsilon(1) > 0$. If ξ_1, ξ_2 satisfies $\Upsilon(\xi) = 0$, then*

(1) $|\xi_{1,2}| < 1$ if $\Upsilon(-1) > 0$ and $A_0 < 1$,

(2) $|\xi_1| < 1$ and $|\xi_2| > 1$ (or $|\xi_1| > 1$ and $|\xi_2| < 1$) if $\Upsilon(-1) < 0$,

(3) $|\xi_{1,2}| > 1$ *if* $\Upsilon(-1) > 0$ *and* $A_0 > 1$*,*

(4) $\xi_1 = -1$ *and* $|\xi_2| \neq 1$ *if* $\Upsilon(-1) = 0$ *and* $A_1 \neq 0, 2$*,*

(5) $\xi_{1,2}$ *are complex and* $|\xi_{1,2}| = 1$ *if* $A_1^2 - 4A_0 < 0$ *and* $A_0 = 1$.

2.1. Topological classification of E_0

Consider

$$\Gamma_0 = \left\{(r, h, k, a, b, d, \epsilon) \in \mathbb{R}_+^7 \middle| \, 0 < \epsilon < 1\right\}.$$

The following result is obtained by applying the Lemma 2.1:

Proposition 2.3. *In* Γ_0*, the trivial fixed point* E_0 *of the model* (1.6) *is a*

(1) *SP if* $0 < \epsilon < \frac{2}{dh}$*,*

(2) *source if* $\epsilon > \frac{2}{dh}$*,*

(3) *NHP if* $\epsilon = \frac{2}{dh}$.

Proof. The Jacobian matrix at E_0 is provided by

$$J(0, 0) = \begin{bmatrix} 1 + \frac{hr}{2} & -\frac{ah}{2} \\ 0 & 1 - dh\epsilon \end{bmatrix}.$$

The eigenvalues of $J(0, 0)$ are $\xi_1 = 1 + \frac{hr}{2}$ and $\xi_2 = 1 - dh\epsilon$.

□

Remark 2.4. *The analysis of the fixed point* E_0 *reveals that it is never stable. This lack of stability has a significant ecological implication: The predator and prey populations cannot go to extinction simultaneously at this fixed point. Instead, the populations may exhibit oscillatory behavior or other forms of non-extinction dynamics.*

2.2. Topological classification of $E_1 = (\sqrt{k}, 0)$

Next, considering the same set Γ_0, we obtain the following result by applying the Lemma 2.1:

Proposition 2.5. *In* Γ_0*, the boundary fixed point* E_1 *of the model* (1.6) *is a*

(1) *sink if* $r < \frac{2}{h}$ *and* $b\sqrt{k} < d < b\sqrt{k} + \frac{2}{h\epsilon}$*,*

(2) *SP if any one of the following is true:*

(a) $r > \frac{2}{h}$ *and* $b\sqrt{k} < d < b\sqrt{k} + \frac{2}{h\epsilon}$,
(b) $r < \frac{2}{h}$ *and either* $d < b\sqrt{k}$ *or* $d > b\sqrt{k} + \frac{2}{h\epsilon}$,

(3) source if $r > \frac{2}{h}$ *and any one of the following is true:*
(a) $d < b\sqrt{k}$,
(b) $d > b\sqrt{k} + \frac{2}{h\epsilon}$,

(4) NHP if any one of the following is true:
(a) $h = \frac{2}{r}$,
(b) $d = b\sqrt{k}$,
(c) $d = b\sqrt{k} + \frac{2}{h\epsilon}$.

Proof. Simple calculations yields

$$J(\sqrt{k}, 0) = \begin{bmatrix} 1 - hr & -\frac{ah}{2} \\ 0 & 1 - dh\epsilon + bh\sqrt{k}\epsilon \end{bmatrix}.$$

The eigenvalues of $J(0,0)$ are $\xi_1 = 1 - hr$ and $\xi_2 = 1 - dh\epsilon + bh\sqrt{k}\epsilon$.

□

Remark 2.6. *The boundary fixed point* $E_1 = (k, 0)$ *refers to a situation in the predator-prey model, where the prey population is at its carrying capacity, meaning it has reached the maximum number of individuals that the environment can support. The predator population, on the other hand, is at zero, signifying that the predators have gone extinct. The stability of the boundary fixed point* E_1 *has significant ecological implications, namely that the predator population can go to extinction and remain extinct as long as the system operates under the conditions that stabilize this fixed point.*

2.3. Topological classification of $E_2 = \left(\frac{d}{b}, \frac{d(-d^2+b^2k)r}{ab^3k}\right)$

We consider the following set:

$$\Gamma_2 = \left\{(r, h, k, a, b, d, \epsilon) \in \mathbb{R}_+^7 \middle| \, 0 < \epsilon < 1, \ k > \frac{d^2}{b^2} \right\}.$$

The Jacobian matrix at E_2 is provided by

$$J(E_2) = \begin{bmatrix} 1 + \frac{rh}{2}(1 - \frac{3d^2}{b^2k}) & -\frac{ah}{2} \\ \frac{dhr\epsilon(-d^2+b^2k)}{ab^2k} & 1 \end{bmatrix}. \tag{2.2}$$

The characteristic polynomial of $J(E_2)$ is provided by

$$\Upsilon(\xi) = \xi^2 + \left(-2 + \frac{rh}{2}(-1 + \frac{3d^2}{b^2k})\right)\xi + \frac{1}{2}\left(2 + rh + dh^2r\epsilon - \frac{d^2hr(3 + dh\epsilon)}{b^2k}\right). \tag{2.3}$$

By simple computations, we obtain

$$\Upsilon(0) = \frac{1}{2}\Big(2 + rh + dh^2 r\epsilon - \frac{d^2hr(3 + dh\epsilon)}{b^2k}\Big),$$
$$\Upsilon(-1) = \frac{1}{2}\Big(8 + 2hr + dh^2 r\epsilon - \frac{d^2hr(6 + dh\epsilon)}{b^2k}\Big),$$
$$\Upsilon(1) = \frac{dh^2(-d^2 + b^2k)r\epsilon}{2b^2k}.$$

It is obvious that $\Upsilon(1) > 0$ in Γ_2. We obtain the following result by applying Lemmas 2.1 and 2.2:

Proposition 2.7. *In Γ_2, the fixed point E_2 is a*

(1) sink if $k < \frac{3d^2}{b^2}$, $h < \frac{-3d^2+b^2k}{d^3\epsilon-b^2dk\epsilon}$, and

$$r < \frac{8b^2k}{6d^2h - 2b^2hk + d^3h^2\epsilon - b^2dh^2k\epsilon},$$

(2) SP if $k < \frac{3d^2}{b^2}$, $h < \frac{-6d^2+2b^2k}{d^3\epsilon-b^2dk\epsilon}$, and

$$r > \frac{8b^2k}{6d^2h - 2b^2hk + d^3h^2\epsilon - b^2dh^2k\epsilon},$$

(3) source if any one of the following is true:

(a) $k \geq \frac{3d^2}{b^2}$,

(b) $k < \frac{3d^2}{b^2}$ and any one of the following is true:

(i) $h \geq \frac{-6d^2+2b^2k}{d^3\epsilon-b^2dk\epsilon}$,

(ii) $\frac{-3d^2+b^2k}{d^3\epsilon-b^2dk\epsilon} < h < \frac{-6d^2+2b^2k}{d^3\epsilon-b^2dk\epsilon}$ and $r < \frac{8b^2k}{6d^2h-2b^2hk+d^3h^2\epsilon-b^2dh^2k\epsilon}$,

(4) NHP if $k < \frac{3d^2}{b^2}$ and any one of the following is true:

(a) $h < \frac{-6d^2+2b^2k}{d^3\epsilon-b^2dk\epsilon}$ and

$$r = \frac{8b^2k}{6d^2h - 2b^2hk + d^3h^2\epsilon - b^2dh^2k\epsilon},$$

(b) $r < \frac{8b^2dk\epsilon(-d^2+b^2k)}{(3d^2-b^2k)^2}$ and $h = \frac{3d^2-b^2k}{d\epsilon(-d^2+b^2k)}$.

Remark 2.8. *The positive fixed point E_2 refers to a situation in the predator-prey model where both the predator and prey populations have non-zero positive values. This implies that both species coexist at non-trivial population levels. The stability of the fixed point E_2 suggests that the predator and prey populations can coexist and persist in the ecosystem under the specified parametric conditions.*

3. Bifurcation analysis

This section discusses the PD and NS bifurcations at the interior fixed point $E_2 = \left(\frac{d}{b}, \frac{d(-d^2+b^2k)r}{ab^3k}\right)$ of the model (1.6). We establish the conditions of existence for the PD and NS bifurcations using the center manifold theorem and bifurcation theory [38, 45–47].

Initially, we explored the PD bifurcation at E_2. To study the PD bifurcation, consider the following set:

$$\Gamma_{PD} = \left\{(r,h,k,a,b,d,\epsilon) \in \mathbb{R}^7_+ \middle| 0 < \epsilon < 1,\ h < \frac{-6d^2 + 2b^2k}{d^3\epsilon - b^2dk\epsilon}, \right.$$
$$\left. k < \frac{3d^2}{b^2},\ r = r_1 := \frac{8b^2k}{6d^2h - 2b^2hk + d^3h^2\epsilon - b^2dh^2k\epsilon}\right\}.$$

Suppose that $(r,h,k,a,b,d,\epsilon) \in \Gamma_{PD}$, and γ be minimal change in r_1. Given a perturbation of model (1.6) as follows:

$$\begin{cases} u_{n+1} = u_n + \frac{h}{2}\left((r_1+\gamma)u_n(1 - \frac{u_n^2}{k}) - av_n\right), \\ v_{n+1} = v_n + \epsilon h v_n(-d + bu_n), \end{cases} \tag{3.1}$$

where γ is a parameter that accounts for minimal changes. In order to translate the fixed point $\left(\frac{d}{b}, \frac{d(-d^2+b^2k)(r_1+\gamma)}{ab^3k}\right)$ to $(0,0)$, we define translation map as follows:

$$a_n = u_n - \frac{d}{b},\ b_n = v_n - \frac{d(-d^2+b^2k)(r_1+\gamma)}{ab^3k}.$$

As a result of this translation map, the system (3.1) transforms to

$$\begin{bmatrix} a_{n+1} \\ b_{n+1} \end{bmatrix} = \begin{bmatrix} m_{11} & m_{12} \\ m_{21} & 1 \end{bmatrix} \begin{bmatrix} a_n \\ b_n \end{bmatrix} + \begin{bmatrix} F(a_n,b_n,\gamma) \\ G(a_n,b_n,\gamma) \end{bmatrix}, \tag{3.2}$$

where

$$m_{11} = \frac{6d^2 - 2b^2k - d^3h\epsilon + b^2dhk\epsilon}{-6d^2 + 2b^2k - d^3h\epsilon + b^2dhk\epsilon},\ m_{12} = -\frac{1}{2}ah,$$
$$m_{21} = -\frac{8d\left(d^2 - b^2k\right)\epsilon}{a\left(6d^2 - 2b^2k + d^3h\epsilon - b^2dhk\epsilon\right)},$$

$$F(a_n,b_n,\gamma) = c_1\gamma a_n + c_2\gamma a_n^2 + c_3a_n^2 + c_4a_n^3 + O((|a_n| + |b_n| + |\gamma|)^4),$$
$$G(a_n,b_n,\gamma) = d_1\gamma a_n + d_2a_nb_n + O((|a_n| + |b_n| + |\gamma|)^4),$$

$$c_1 = \frac{1}{2}h\left(1 - \frac{3d^2}{b^2k}\right),\ c_2 = -\frac{3dh}{2bk},\ c_3 = \frac{12bd}{-6d^2 + 2b^2k - d^3h\epsilon + b^2dhk\epsilon},$$

$$c_4 = \frac{4b^2}{-6d^2+2b^2k-d^3h\epsilon+b^2dhk\epsilon},\ d_1 = \frac{dh\left(-d^2+b^2k\right)\epsilon}{ab^2k},\ d_2 = bh\epsilon.$$

For $r_1 = \frac{8b^2k}{6d^2h-2b^2hk+d^3h^2\epsilon-b^2dh^2k\epsilon}$, the eigenvalues of $J(E_2)$ are $\xi_1 = -1$ and

$$\xi_2 = \frac{6d^2-2b^2k+3d^3h\epsilon-3b^2dhk\epsilon}{6d^2-2b^2k+d^3h\epsilon-b^2dhk\epsilon}.$$

Let

$$T = \begin{bmatrix} \frac{6ad^2-2ab^2k+ad^3h\epsilon-ab^2dhk\epsilon}{4d\epsilon(d^2-b^2k)} & -\frac{ah}{4} \\ 1 & 1 \end{bmatrix}.$$

Under the following transformation

$$\begin{bmatrix} a_n \\ b_n \end{bmatrix} = T \begin{bmatrix} e_n \\ f_n \end{bmatrix}, \tag{3.3}$$

the system (3.2) transforms to

$$\begin{bmatrix} e_{n+1} \\ f_{n+1} \end{bmatrix} = \begin{bmatrix} -1 & 0 \\ 0 & \xi_2 \end{bmatrix} \begin{bmatrix} e_n \\ f_n \end{bmatrix} + \begin{bmatrix} F(e_n, f_n, \gamma) \\ G(e_n, f_n, \gamma) \end{bmatrix}, \tag{3.4}$$

where

$$\begin{aligned} F(e_n, f_n, \gamma) &= D_1 f_n^3 + D_2 e_n^3 + D_3 e_n f_n^2 + D_4 e_n f_n + D_5 f_n \gamma + D_6 e_n \gamma + D_7 e_n^2 \gamma + D_8 e_n^2 f_n \\ &\quad + D_9 e_n f_n \gamma + D_{10} e_n^2 + D_{11} f_n^2 + O((|e_n| + |f_n| + |\gamma|)^4), \\ G(e_n, f_n, \gamma) &= E_1 e_n f_n^2 + E_2 f_n^3 + E_3 e_n^3 + E_4 f_n \gamma + E_5 e_n f_n \gamma + E_6 e_n \gamma + E_7 e_n^2 \gamma + E_8 e_n^2 f_n \\ &\quad + E_9 e_n f_n + E_{10} e_n^2 + E_{11} f_n^2 + O((|e_n| + |f_n| + |\gamma|)^4), \end{aligned}$$

$$\begin{aligned} D_1 &= \frac{3a^2b^2h^2}{24d^2-8b^2k+8d^3h\epsilon-8b^2dhk\epsilon}, \\ D_2 &= \frac{a^2b^2dh^3\left(-d^2+b^2k\right)\epsilon}{8\left(6d^2-2b^2k+d^3h\epsilon-b^2dhk\epsilon\right)\left(3d^2-b^2k+d^3h\epsilon-b^2dhk\epsilon\right)}, \end{aligned}$$

$$D_3 = \frac{a^2b^2\left(6d^2-2b^2k+d^3h\epsilon-b^2dhk\epsilon\right)^2}{8d^2\left(d^2-b^2k\right)^2\epsilon^2\left(3d^2-b^2k+d^3h\epsilon-b^2dhk\epsilon\right)}, D_4 = \frac{3ad^2h^3\left(-d^2+b^2k\right)\epsilon}{8bk\left(-3d^2+b^2k-d^3h\epsilon+b^2dhk\epsilon\right)},$$

$$D_5 = -\frac{d^2h^3\left(d^2-b^2k\right)^2\ \epsilon^2}{8b^2k\left(-3d^2+b^2k-d^3h\epsilon+b^2dhk\epsilon\right)}, D_6 = \frac{3adh^2\left(6d^2-2b^2k+d^3h\epsilon-b^2dhk\epsilon\right)}{8bk\left(-3d^2+b^2k-d^3h\epsilon+b^2dhk\epsilon\right)},$$

$$D_7 = \frac{dh^2\left(d^2 - b^2k\right)\,\epsilon\left(6d^2 - 2b^2k + d^3h\epsilon - b^2dhk\epsilon\right)}{8b^2k\,(-3d^2 + b^2k - d^3h\epsilon + b^2dhk\epsilon)},$$

$$D_8 = \frac{3a^2b^2h\left(-6d^2 + 2b^2k - d^3h\epsilon + b^2dhk\epsilon\right)}{8d\,(d^2 - b^2k)\,\epsilon\,(3d^2 - b^2k + d^3h\epsilon - b^2dhk\epsilon)},$$

$$D_9 = \frac{abh\left(6d^4 + 2b^4k^2 + 3d^5h\epsilon - 4b^2d^3hk\epsilon + b^4dhk^2\epsilon\right)}{4d\,(d^2 - b^2k)\,(3d^2 - b^2k + d^3h\epsilon - b^2dhk\epsilon)},$$

$$\begin{aligned}
D_{10} &= \frac{ab\left(-6d^2 + 2b^2k - d^3h\epsilon + b^2dhk\epsilon\right)\left(-6d^2h\epsilon + 2b^2hk\epsilon - d^3h^2\epsilon^2 + d\left(-12 + b^2h^2k\epsilon^2\right)\right)}{8d\,(d^2 - b^2)\,\epsilon\,(3d^2 - b^2k + d^3h\epsilon - b^2dhk\epsilon)},\\
D_{11} &= -\frac{abdh^2(-d^2 + b^2k)\epsilon(-6d^2h\epsilon + 2b^2hk\epsilon - d^3h^2\epsilon^2 + d(-12 + b^2h^2k\epsilon^2))}{8(6d^2 - 2b^2k + d^3h\epsilon - b^2dhk\epsilon)(3d^2 - b^2k + d^3h\epsilon - b^2dhk\epsilon)},\\
E_1 &= -\frac{a^2b^2dh^3\left(-d^2 + b^2k\right)\epsilon}{8\,(6d^2 - 2b^2k + d^3h\epsilon - b^2dhk\epsilon)\,(3d^2 - b^2k + d^3h\epsilon - b^2dhk\epsilon)},\\
E_2 &= -\frac{a^2b^2\left(6d^2 - 2b^2k + d^3h\epsilon - b^2dhk\epsilon\right)^2}{8d^2\,(d^2 - b^2k)^2\,\epsilon^2\,(3d^2 - b^2k + d^3h\epsilon - b^2dhk\epsilon)}, E_3 = \frac{3a^2b^2h^2}{8\,(-3d^2 + b^2k - d^3h\epsilon + b^2dhk\epsilon)},\\
E_4 &= \frac{3ad^2h^3\left(d^2 - b^2k\right)\,\epsilon}{8bk\,(-3d^2 + b^2k - d^3h\epsilon + b^2dhk\epsilon)}, E_5 = \frac{abh\left(-12d - 3d^2h\epsilon + b^2hk\epsilon\right)}{4\,(-3d^2 + b^2k - d^3h\epsilon + b^2dhk\epsilon)},\\
E_6 &= -\frac{dh^2\left(d^2 - b^2k\right)\epsilon\left(6d^2 - 2b^2k + d^3h\epsilon - b^2dhk\epsilon\right)}{8b^2k\,(-3d^2 + b^2k - d^3h\epsilon + b^2dhk\epsilon)}, E_7 = \frac{h\left(6d^2 - 2b^2k + d^3h\epsilon - b^2dhk\epsilon\right)^2}{8b^2k\,(-3d^2 + b^2k - d^3h\epsilon + b^2dhk\epsilon)},\\
E_8 &= -\frac{3a^2b^2h\left(-6d^2 + 2b^2k - d^3h\epsilon + b^2dhk\epsilon\right)}{8d\,(d^2 - b^2k)\,\epsilon\,(3d^2 - b^2k + d^3h\epsilon - b^2dhk\epsilon)}, E_9 = \frac{3adh^2\left(-6d^2 + 2b^2k - d^3h\epsilon + b^2dhk\epsilon\right)}{8bk\,(-3d^2 + b^2k - d^3h\epsilon + b^2dhk\epsilon)},
\end{aligned}$$

$$\begin{aligned}
E_{10} &= \frac{ab\left(-6d^2 + 2b^2k - d^3h\epsilon + b^2dhk\epsilon\right)\left(12 - d^2h^2\epsilon^2 + b^2h^2k\epsilon^2\right)}{8\,(d^2 - b^2k)\,\epsilon\,(3d^2 - b^2k + d^3h\epsilon - b^2dhk\epsilon)},\\
E_{11} &= -\frac{abdh^2\left(-d^2 + b^2k\right)\epsilon\left(-6d^2h\epsilon + 2b^2hk\epsilon - d^3h^2\epsilon^2 + d\left(-12 + b^2h^2k\epsilon^2\right)\right)}{8\,(6d^2 - 2b^2k + d^3h\epsilon - b^2dhk\epsilon)\,(3d^2 - b^2k + d^3h\epsilon - b^2dhk\epsilon)}.
\end{aligned}$$

The local center manifold W^C of system (3.4) at the origin can be obtained using the center manifold theorem as shown below:

$$W^C = \left\{(e_n, f_n, \gamma) \in \mathbb{R}^3 \middle| f_n = c_1e_n^2 + c_2e_n\gamma + c_3\gamma^2 + O((|e_n| + |\gamma|)^3)\right\},$$

where

$$c_1 = \frac{E_{10}}{1-\xi_2},\ c_2 = -\frac{E_6}{1+\xi_2},\ c_3 = 0.$$

Thus, the center manifold-restricted system (3.4) is given by

$$\tilde{F} : e_{n+1} = -e_n + D_2 e_n^3 + D_6 e_n \gamma + D_7 e_n^2 \gamma + D_{10} e_n^2 + D_4\Big(-\frac{E_6 e_n \gamma}{1+\xi_2} + \frac{E_{10} e_n^2}{1-\xi_2}\Big) e_n. \tag{3.5}$$

For PD bifurcation in map (3.5), the values of the two expressions below must not be zero.

$$l_1 = \tilde{F}_\gamma \tilde{F}_{e_n e_n} + 2\tilde{F}_{e_n \gamma}\Big|_{(0,0)},\ l_2 = \frac{1}{2}(\tilde{F}_{e_n e_n})^2 + \frac{1}{3}\tilde{F}_{e_n e_n e_n}\Big|_{(0,0)}.$$

From simple computations, we obtain

$$l_1 = 2D_6 = \frac{h\Big(6d^2 - 2b^2k + d^3h\epsilon - b^2dhk\epsilon\Big)^2}{4b^2k\left(-3d^2 + b^2k - d^3h\epsilon + b^2dhk\epsilon\right)}, \tag{3.6}$$

and

$$l_2 = -\frac{a^2b^2\Big(6d^2 - 2b^2k + d^3h\epsilon - b^2dhk\epsilon\Big)^2\Big(8 + 6d^2h^2\epsilon^2 - 2b^2h^2k\epsilon^2 - d^3h^3\epsilon^3 + dh\epsilon\Big(36 + b^2h^2k\epsilon^2\Big)\Big)}{32d^2\left(d^2 - b^2k\right)^2\epsilon^2\left(3d^2 - b^2k + d^3h\epsilon - b^2dhk\epsilon\right)}. \tag{3.7}$$

The following result is drawn from the calculations above:

Theorem 3.1. *Suppose that* $(r, h, k, a, b, d, \epsilon) \in \Gamma_{PD}$. *The model* (1.6) *undergoes PD bifurcation at the positive fixed point* E_2 *if* l_1, l_2 *defined in* (3.6) *and* (3.7) *are nonzero and* r *varies in a close neighborhood of* $r_1 = \frac{8b^2k}{6d^2h - 2b^2hk + d^3h^2\epsilon - b^2dh^2k\epsilon}$. *Furthermore, if* $l_2 > 0$ *(respectively* $l_2 < 0$*), then the period-2 orbits that bifurcate from* E_2 *are stable (respectively, unstable).*

Next, we studied NS bifurcation about the positive fixed point $E_2 = \left(\frac{d}{b}, \frac{d(-d^2+b^2k)r}{ab^3k}\right)$ of the model (1.6). To study the NS bifurcation, consider the following set:

$$\Gamma_{NS} = \Big\{(r, h, k, a, b, d, \epsilon) \in \mathbb{R}_+^7 \Big|\ 0 < \epsilon < 1,\ r < \frac{8b^2dk\epsilon(-d^2 + b^2k)}{(3d^2 - b^2k)^2},$$
$$k < \frac{3d^2}{b^2},\ h = h_1 := \frac{3d^2 - b^2k}{d\epsilon(-d^2 + b^2k)}\Big\}.$$

Suppose that $(r, h, k, a, b, d, \epsilon) \in \Gamma_{NS}$, and δ be minimal change in h, We take into account the following change to the model (1.6):

$$\begin{cases} u_{n+1} = u_n + \frac{(h_1+\delta)}{2}\Big(ru_n(1 - \frac{u_n^2}{k}) - av_n\Big), \\ v_{n+1} = v_n + \epsilon(h_1 + \delta)v_n(-d + bu_n). \end{cases} \tag{3.8}$$

In order to shift the fixed point $\left(\frac{d}{b}, \frac{d(-d^2+b^2k)r}{ab^3k}\right)$ to $(0,0)$, we define the translation map as follows:

$$a_n = u_n - \frac{d}{b},\ b_n = v_n - \frac{d(-d^2+b^2k)r}{ab^3k}.$$

As a result of this translation map, the system (3.8) transforms to

$$\begin{bmatrix} a_{n+1} \\ b_{n+1} \end{bmatrix} = \begin{bmatrix} l_{11} & l_{12} \\ l_{21} & 1 \end{bmatrix} \begin{bmatrix} a_n \\ b_n \end{bmatrix} + \begin{bmatrix} F(a_n, b_n) \\ G(a_n, b_n) \end{bmatrix}, \tag{3.9}$$

where

$$\begin{aligned} l_{11} &= 1 + \frac{1}{2}\left(r - \frac{3d^2r}{b^2k}\right)\left(\delta + \frac{-3d^2+b^2k}{d^3\epsilon - b^2dk\epsilon}\right), \\ l_{12} &= -\frac{1}{2}a\left(\delta + \frac{-3d^2+b^2k}{d^3\epsilon - b^2dk\epsilon}\right), \\ l_{21} &= \frac{r\left(3d^2 - b^2k - d^3\delta\epsilon + b^2dk\delta\epsilon\right)}{ab^2k}, \end{aligned}$$

$$\begin{aligned} F(a_n, b_n) &= -\frac{3dr\left(\delta + \frac{-3d^2+b^2k}{d^3\epsilon - b^2dk\epsilon}\right)}{2bk}a_n^2 - \frac{r\left(\delta + \frac{-3d^2+b^2k}{d^3\epsilon - b^2dk\epsilon}\right)}{2k}a_n^3 + O((|a_n| + |b_n| + |\delta|)^4), \\ G(a_n, b_n) &= b\epsilon\left(\delta + \frac{-3d^2+b^2k}{d^3\epsilon - b^2dk\epsilon}\right)a_nb_n + O((|a_n| + |b_n| + |\delta|)^4). \end{aligned}$$

Let

$$\xi^2 - \alpha(\delta)\xi + \beta(\delta) = 0, \tag{3.10}$$

be the characteristic equation of the Jacobian matrix for system (3.9) at the point $(0,0)$, where

$$\begin{aligned} \alpha(\delta) &= -\frac{9d^4r - 6b^2d^2kr + b^4k^2r - 3d^5r\delta\epsilon + 4b^2d^3k(1+r\delta)\epsilon - b^4dk^2(4+r\delta)\epsilon}{2b^2dk\left(-d^2+b^2k\right)\epsilon}, \\ \beta(\delta) &= \frac{1}{2}\left(2 + \frac{d^2r\delta(3-d\delta\epsilon)}{b^2k} + r\delta(-1+d\delta\epsilon)\right). \end{aligned}$$

The Eq (3.10) roots are complex that have the property $|\xi_{1,2}| = 1$, which are given by

$$\xi_{1,2} = \frac{\alpha(\delta) \pm i\sqrt{4\beta(\delta) - \alpha^2(\delta)}}{2}.$$

By computations, we obtain

$$|\xi_1| = |\xi_2| = \sqrt{\beta(\delta)}$$

and

$$\left(\frac{d|\xi_1|}{d\delta}\right)_{\delta=0} = \left(\frac{d|\xi_2|}{d\delta}\right)_{\delta=0} = \frac{r}{4}\left(-1 + \frac{3d^2}{b^2k}\right) > 0.$$

Moreover, it is required that $\xi_1^p, \xi_2^p \neq 1$ for $p \in \{1,2,3,4\}$ at $\delta = 0$, which is equivalent to $\alpha(0) \notin \{-2,0,1,2\}$. By simple calculations, it is obtained that

$$\alpha(0) = 2 - \frac{r(3d^2 - b^2k)^2}{2b^2dk\epsilon(b^2k - d^2)}.$$

Clearly, $\alpha(0) \neq 2$. Since $r < \frac{8b^2dk\epsilon(-d^2+b^2k)}{(3d^2-b^2k)^2}$ in Γ_{NS}, therefore $\alpha(0) > -2$. We only require that $\alpha(0) \neq 0, 1$, which leads to the following:

$$r \neq \frac{4b^2dk\epsilon(-d^2 + b^2k)}{(-3d^2 + b^2k)^2}, \frac{2b^2dk\epsilon(-d^2 + b^2k)}{(-3d^2 + b^2k)^2}.$$

Subsequently, the transformation employed to convert the linear part of Eq (3.9) into canonical form at $\delta = 0$ is as follows:

$$\begin{bmatrix} a_n \\ b_n \end{bmatrix} = \begin{bmatrix} \frac{3ad^2 - ab^2k}{2d^3\epsilon - 2b^2dk\epsilon} & 0 \\ \frac{\left(-3d^2+b^2k\right)^2 r}{4b^2dk\left(-d^2+b^2k\right)\epsilon} & k_{22} \end{bmatrix} \begin{bmatrix} e_n \\ f_n \end{bmatrix}, \tag{3.11}$$

where

$$k_{22} = -\frac{1}{2}\sqrt{4 - \frac{\left(9d^4r - 6b^2d^2kr + b^4k^2r + 4b^2d^3k\epsilon - 4b^4dk^2\epsilon\right)^2}{4b^4d^2k^2\left(d^2 - b^2k\right)^2\epsilon^2}}.$$

When (3.9) is transformed by (3.11), the resulting system is

$$\begin{bmatrix} e_{n+1} \\ f_{n+1} \end{bmatrix} = \begin{bmatrix} \mu & -\nu \\ \nu & \mu \end{bmatrix} \begin{bmatrix} e_n \\ f_n \end{bmatrix} + \begin{bmatrix} F(e_n, f_n) \\ G(e_n, f_n) \end{bmatrix}, \tag{3.12}$$

where

$$\begin{aligned} \mu &= \frac{9d^4r - 6b^2d^2kr + b^4k^2r + 4b^2d^3k\epsilon - 4b^4dk^2\epsilon}{4b^2d^3k\epsilon - 4b^4dk^2\epsilon}, \\ \nu &= \frac{\left(-3d^2 + b^2k\right)\sqrt{r\left(-9d^4r + 6b^2d^2kr - b^4k^2r - 8b^2d^3k\epsilon + 8b^4dk^2\epsilon\right)}}{4(b^2dk\left(d^2 - b^2k\right)\epsilon)}, \end{aligned}$$

$$F(e_n, f_n) = -\frac{a^2\left(-3d^2 + b^2k\right)^3 re_n^3}{8k\left(d^3\epsilon - b^2dk\epsilon\right)^3} + \frac{3ad\left(-3d^2 + b^2k\right)^2 re_n^2}{4bk\left(d^3\epsilon - b^2dk\epsilon\right)^2} + O((|e_n| + |f_n|)^4),$$

$$\begin{aligned} G(e_n, f_n) = &-\frac{ab\left(-3d^2 + b^2k\right)^2 \epsilon e_n f_n}{2\left(d^3\epsilon - b^2dk\epsilon\right)^2} + \frac{a^2\left(-3d^2 + b^2k\right)^5 r^2 e_n^3}{32b^2d^4k^2\left(d^2 - b^2k\right)^4\epsilon^4\nu} \\ &+ \frac{a\left(-3d^2 + b^2k\right)^4 re_n^2\left(3dr + 2b^2k\epsilon\right)}{16b^3d^3k^2\left(-d^2 + b^2k\right)^3\epsilon^3\nu} + O((|e_n| + |f_n|)^4). \end{aligned}$$

The following number, L, explains how the invariant curve appears in a model going through NS bifurcation:

$$L = \left(\left[-Re\left(\frac{(1-2\xi_1)\xi_2^2}{1-\xi_1} \eta_{20}\eta_{11} \right) - \frac{1}{2}|\eta_{11}|^2 - |\eta_{02}|^2 + Re(\xi_2\eta_{21}) \right] \right)_{\delta=0},$$

where

$$\begin{aligned}
\eta_{20} &= \frac{1}{8}\left[F_{e_ne_n} - F_{f_nf_n} + 2G_{e_nf_n} + i(G_{e_ne_n} - G_{f_nf_n} - 2F_{e_nf_n}) \right],\\
\eta_{11} &= \frac{1}{4}\left[F_{e_ne_n} + F_{f_nf_n} + i(G_{e_ne_n} + G_{f_nf_n}) \right],\\
\eta_{02} &= \frac{1}{8}\left[F_{e_ne_n} - F_{f_nf_n} - 2G_{e_nf_n} + i(G_{e_ne_n} - G_{f_nf_n} + 2F_{e_nf_n}) \right],\\
\eta_{21} &= \frac{1}{16}\left[F_{e_ne_ne_n} + F_{e_nf_nf_n} + G_{e_ne_nf_n} + G_{f_nf_nf_n} + i(G_{e_ne_ne_n} + G_{e_nf_nf_n} - F_{e_ne_nf_n} - F_{f_nf_nf_n}) \right].
\end{aligned}$$

Based on the analytical approach discussed earlier, we can formulate the following theorem as a result:

Theorem 3.2. *Assume that* $(r, h, k, a, b, d, \epsilon) \in \Gamma_{NS}$. *When the parameter h differs in a small neighborhood of* $h_1 = \frac{3d^2-b^2k}{d\epsilon(-d^2+b^2k)}$, *the model* (1.6) *goes through NS bifurcation at* E_2 *if* $L \neq 0$ *and*

$$r \neq \frac{4b^2dk\epsilon(-d^2+b^2k)}{(-3d^2+b^2k)^2}, \frac{2b^2dk\epsilon(-d^2+b^2k)}{(-3d^2+b^2k)^2}.$$

Furthermore, in the case of L being negative, an attracting invariant curve emerges from E_2 *when h exceeds* h_1, *while in the case of L being positive, a distancing invariant curve emerges from* E_2 *when h is less than* h_1.

4. Chaos control

Chaos control techniques are widely utilized in numerous fields of applied research and engineering. In the context of dynamical models, it is preferable to optimize the model based on specific performance criteria while simultaneously minimizing the occurrence of chaotic behavior. In the field of mathematical biology, bifurcations and unstable fluctuations have conventionally been regarded as unfavorable phenomena due to their hindrance to the growth of a biological population, and thus, should be avoided at any expense. The feasibility of devising a controller capable of modifying the bifurcation properties of a specific nonlinear dynamical system in order to mitigate the chaotic behavior arising from PD and NS bifurcations is worth exploring. Consequently, specific dynamical characteristics that are sought after can be achieved. The hybrid control method [48] is employed to regulate chaos in the model (1.6) via both types of bifurcation effects. We consider the controlled model shown below:

$$\begin{cases} u_{n+1} = \rho\Big(u_n + \frac{h}{2}\Big(ru_n(1-\frac{u_n^2}{k}) - av_n\Big)\Big) + (1-\rho)u_n,\\ v_{n+1} = \rho\Big(v_n + \epsilon hv_n(-d+bu_n)\Big) + (1-\rho)v_n, \end{cases} \tag{4.1}$$

where $\rho \in (0, 1)$. Upon considering the set Γ_2, it can be observed that the fixed points of the controlled model represented by system (4.1) coincide with those of the uncontrolled model denoted by system (1.6). The Jacobian matrix of (4.1) at $E_2 = \left(\frac{d}{b}, \frac{d(-d^2+b^2k)r}{ab^3k}\right)$ is provided by

$$J(E_2) = \begin{bmatrix} j_{11} & j_{12} \\ j_{21} & 1 \end{bmatrix},$$

where

$$\begin{aligned} j_{11} &= 1 + \frac{1}{2}h\left(1 - \frac{3d^2}{b^2k}\right)r\rho,\ j_{12} = -\frac{1}{2}ah\rho, \\ j_{21} &= \frac{dh\left(-d^2 + b^2k\right)r\epsilon\rho}{ab^2k}. \end{aligned}$$

Let

$$\Upsilon(\xi) = \xi^2 + B_1\xi + B_0, \tag{4.2}$$

be the characteristic polynomial of $J(E_3)$, where

$$\begin{aligned} B_1 &= -2 + \frac{1}{2}h\left(-1 + \frac{3d^2}{b^2k}\right)r\rho, \\ B_0 &= \frac{1}{2}\left(2 + hr\rho + dh^2r\epsilon\rho^2 - \frac{d^2hr\rho(3 + dh\epsilon\rho)}{b^2k}\right). \end{aligned}$$

By simple computations, we obtain

$$\begin{aligned} \Upsilon(1) &= \frac{dh^2\left(-d^2 + b^2k\right)r\epsilon\rho^2}{2b^2k}, \\ \Upsilon(-1) &= \frac{1}{2}\left(8 + 2hr\rho + dh^2r\epsilon\rho^2 - \frac{d^2hr\rho(6 + dh\epsilon\rho)}{b^2k}\right), \\ \Upsilon(0) &= \frac{1}{2}\left(2 + hr\rho + dh^2r\epsilon\rho^2 - \frac{d^2hr\rho(3 + dh\epsilon\rho)}{b^2k}\right). \end{aligned}$$

It is evident that the value of $\Upsilon(1)$ is greater than zero. According to Lemma 2.2, the fixed point E_2 of the model (1.6) exhibits local asymptotic stability under the conditions that $\Upsilon(1) > 0$, $\Upsilon(-1) > 0$ and $\Upsilon(0) < 1$. Thus, we obtain the following result:

Theorem 4.1. *Consider the set* Γ_2. *If* $\rho \in (0, 1)$*, then the fixed point* E_2 *of the controlled model* (4.1) *is LAS if* $k < \frac{3d^2}{b^2}$, $h < \frac{-3d^2+b^2k}{d^3\epsilon\rho - b^2dk\epsilon\rho}$, *and*

$$r < \frac{8b^2k}{h\rho\left(6d^2 - 2b^2k + d^3h\epsilon\rho - b^2dhk\epsilon\rho\right)}.$$

5. Numerical simulation

This section provides some numerical simulations to verify our theoretical results.

5.1. NS bifurcation analysis by varying h

We consider the following parameters set:

$$r = 1.5, h = 1.5, k = 0.95, a = 1, b = 0.9, d = 0.6, \epsilon = 0.8$$

with the initial conditions $(u_0, v_0) = (0.6, 0.5)$ for the model (1.6). At this set, the positive fixed point is $E_2 = (0.666667, 0.532164)$ and the Jacobian matrix at E_2 is provided by

$$J(0.666667, 0.532164) = \begin{bmatrix} 0.546053 & -0.75 \\ 0.574737 & 1 \end{bmatrix}.$$

The eigenvalues of $J(0.666667, 0.532164)$ are $\xi_{1,2} = 0.773026 \pm 0.616065i$ with $|\xi_{1,2}| < 1$. It indicates that E_2 is LAS. Due to NS bifurcation, the fixed point E_2 might destabilize when the bifurcation parameter h grows. At $h = \frac{3d^2-b^2k}{d\epsilon(-d^2+b^2k)} \approx 1.57967$, the fixed point is $E_2 \approx (0.666667, 0.532164)$ and the Jacobian matrix $J(E_2)$ is provided by

$$J(0.666667, 0.532164) = \begin{bmatrix} 0.521942 & -0.789835 \\ 0.605263 & 1 \end{bmatrix}.$$

The eigenvalues of $J(0.666667, 0.532164)$ are $\xi_{1,2} = 0.760971 \pm 0.648786i$ with $|\xi_{1,2}| = 1$. It verifies the existence of NS bifurcation at E_2 in the model (1.6). Figure 1a,1b depicts bifurcation diagrams for $h \in [1.5, 2.65]$.

The fixed point E_2 is a sink for these parameters' values if $h < 1.57967$. Figure 2a–2f depicts phase portraits of the model (1.6) for some values of h. The figures depict that the fixed point E_2 is a sink for $h < 1.57967$ but losses stability at $h \approx 1.57967$, where the model (1.6) undergoes NS bifurcation. For $h \geq 1.57967$, there is a smooth invariant curve whose radius increases as h increases. By increasing h, the invariant curve disappears abruptly, and a periodic orbit appears; however, the invariant curve reappears in place of the periodic orbit. Large values of h result in the apparition of a strange chaotic attractor. Maximum Lyapunov exponent (MLE) graph of model (1.6) is depicted in Figure 1c.

Next, for the controlled model (4.1), we consider the following parameters set:

$$r = 1.5, k = 0.95, a = 1, b = 0.9, d = 0.6, \epsilon = 0.8$$

with the initial conditions $(u_0, v_0) = (0.6, 0.5)$. We selected the same parameter set we used for NS bifurcation analysis. First, we select the control parameter as $\rho = 0.9$. For this control parameter value, the model (4.1) experiences NS bifurcation for $h \geq 1.75519$. The NS bifurcation has been delayed in the controlled model (4.1). See Figure 3.

Next, we select the control parameter as $\rho = 0.7$. For this control parameter value, the model (4.1) experiences NS bifurcation for $h \geq 2.25667$. It means that the small values of the control parameter ρ result in more delay in the NS bifurcation in the model. See Figure 4.

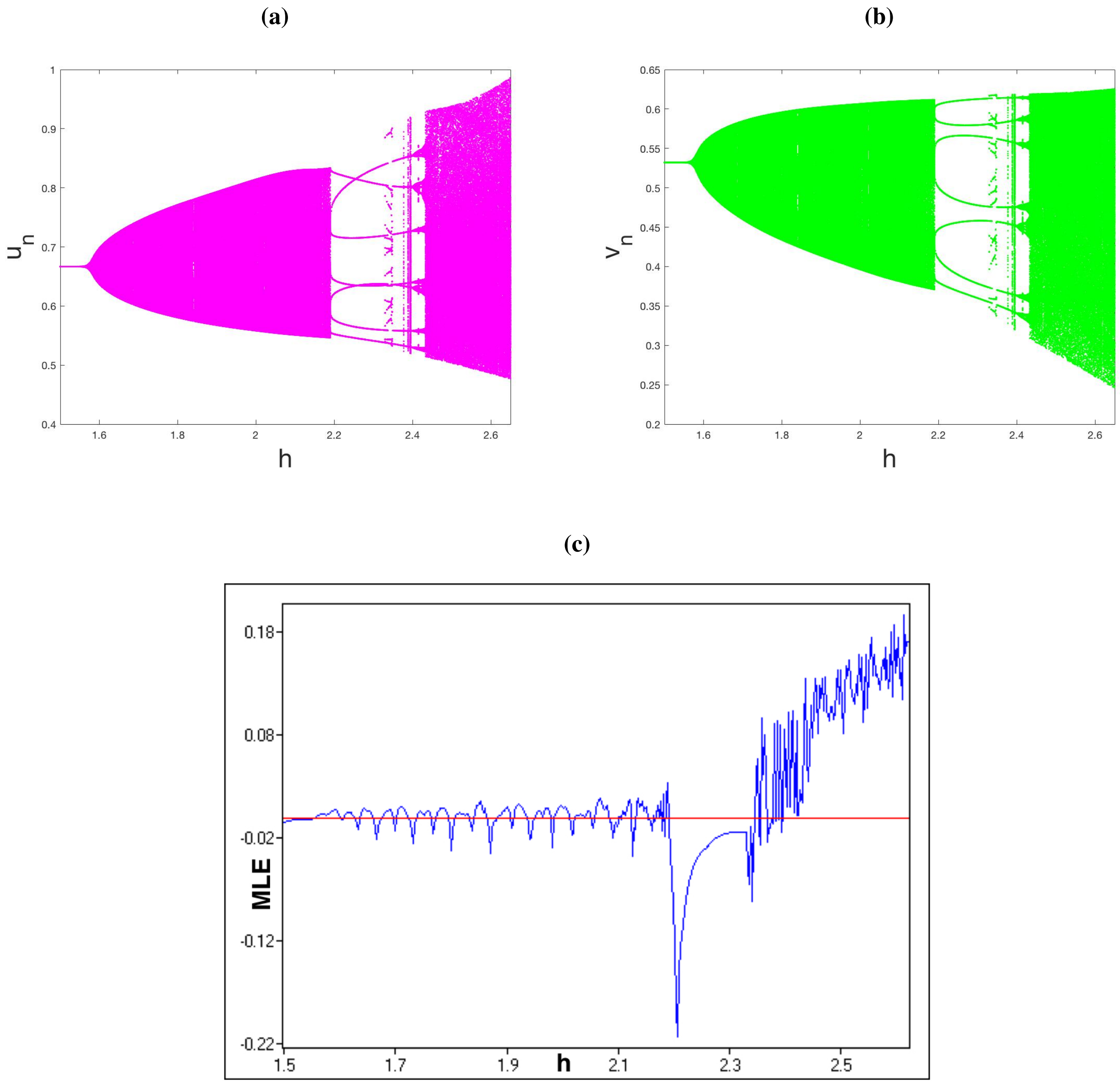

Figure 1. Bifurcation diagrams and MLE graph of (1.6) for $r = 1.5, k = 0.95, a = 1, b = 0.9, d = 0.6, \epsilon = 0.8, u_0 = 0.6,\ v_0 = 0.5, h \in [1.5, 2.65]$.

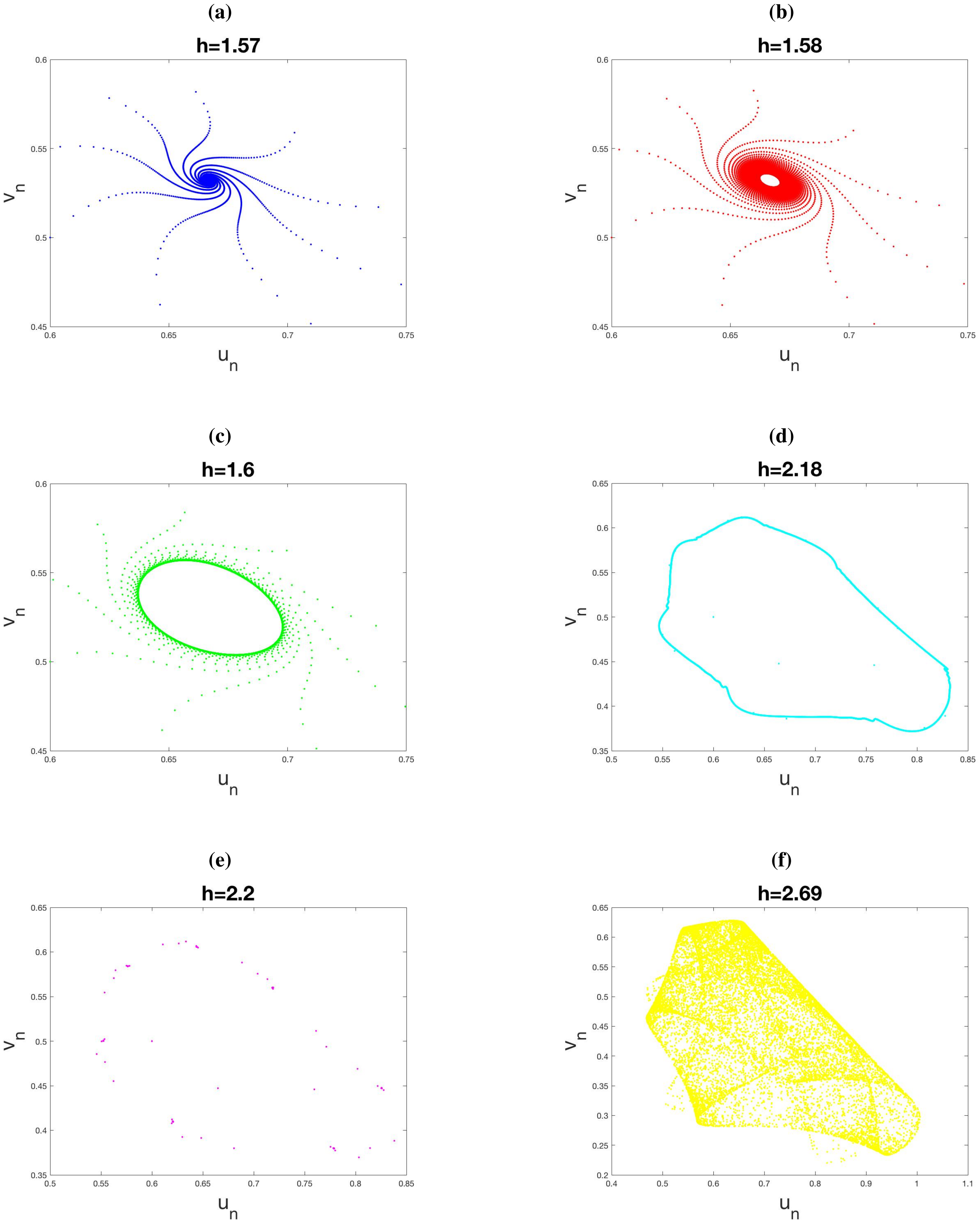

Figure 2. Phase portraits of (1.6) for $r = 1.5, k = 0.95, a = 1, b = 0.9, d = 0.6, \epsilon = 0.8, u_0 = 0.6,\ v_0 = 0.5, h \in \{1.57, 1.58, 1.6, 2.18, 2.2, 2.69\}$.

(a) **(b)**

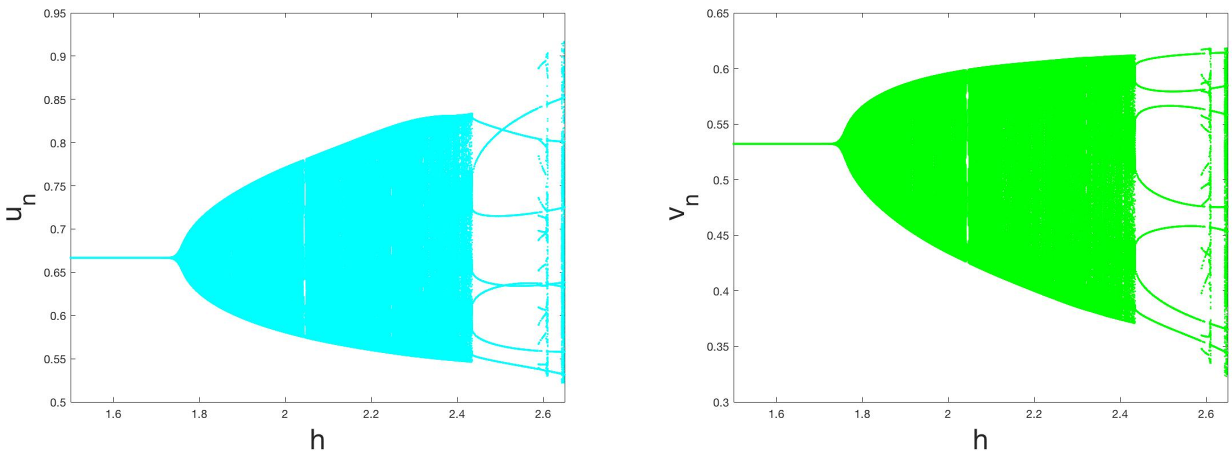

Figure 3. Bifurcation diagrams of (4.1) for $r = 1.5, k = 0.95, a = 1, b = 0.9, d = 0.6, \epsilon = 0.8, \rho = 0.9, u_0 = 0.6,\ v_0 = 0.5, h \in [1.5, 2.65]$.

(a) **(b)**

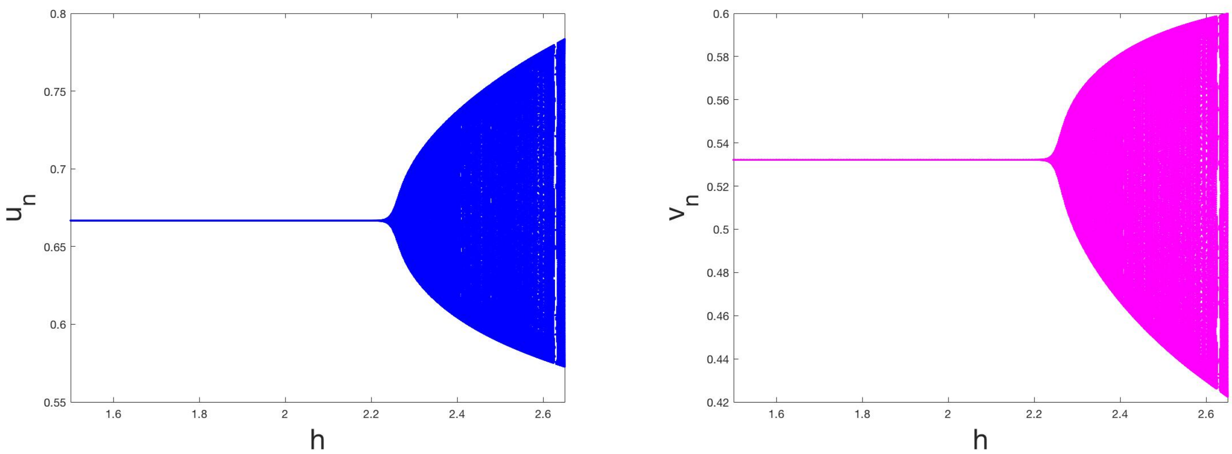

Figure 4. Bifurcation diagrams of (4.1) for $r = 1.5, k = 0.95, a = 1, b = 0.9, d = 0.6, \epsilon = 0.8, \rho = 0.7, u_0 = 0.6,\ v_0 = 0.5, h \in [1.5, 2.65]$.

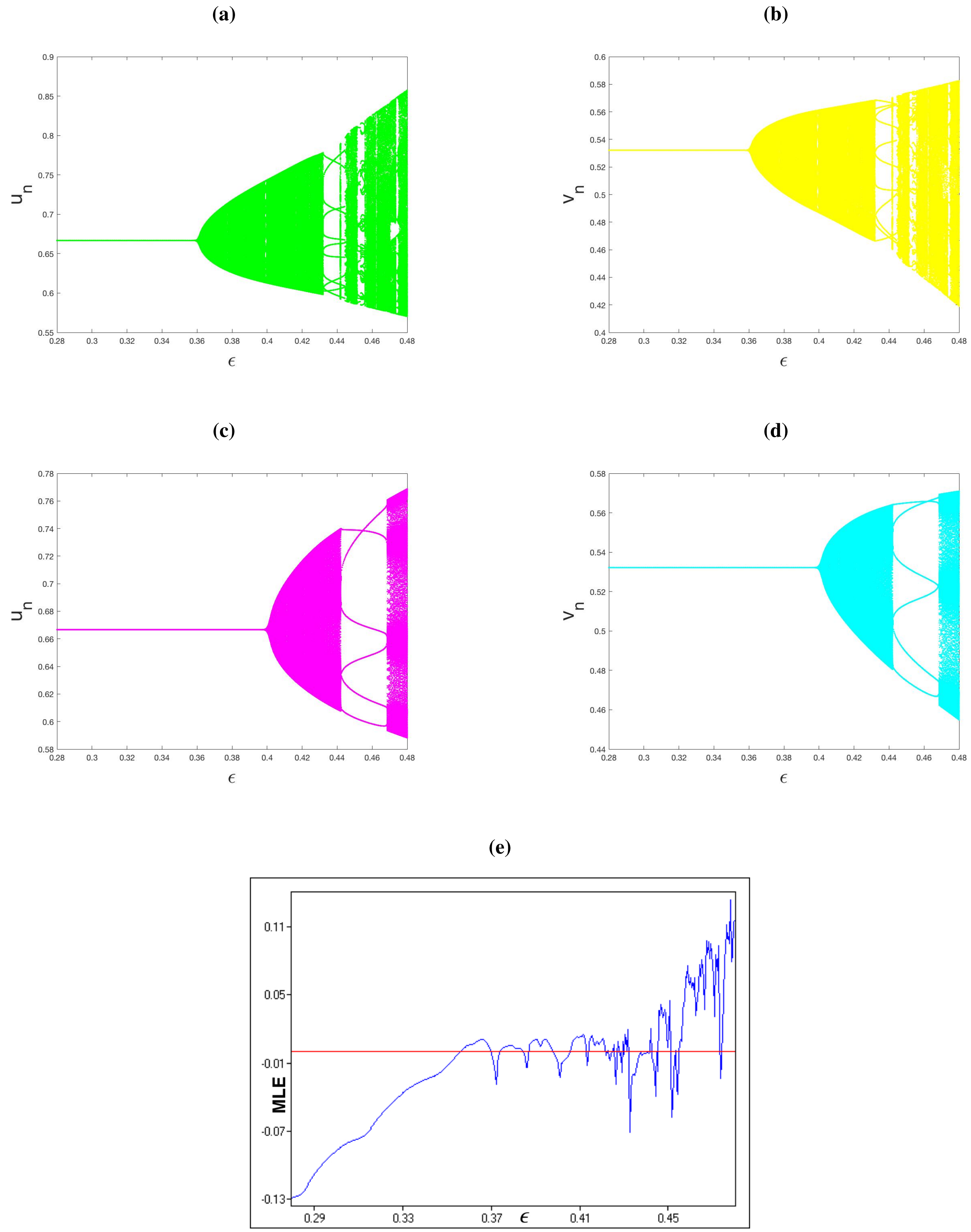

Figure 5. Bifurcation diagrams of (1.6), (4.1) and MLE graph of (1.6) for $\rho = 0.90, a = 1, b = 0.9, d = 0.6, r = 1.5, h = 3.5, k = 0.95, u_0 = 0.6, v_0 = 0.5$, and $\epsilon \in [0.28, 0.48]$.

5.2. NS Bifurcation analysis by varying ϵ

We examine NS bifurcation at E_2 using ϵ as a bifurcation parameter, varying ϵ in the range $0.28 < \epsilon < 0.48$ and setting $a = 1, b = 0.9, d = 0.6, r = 1.5, h = 3.5, k = 0.95, u_0 = 0.6, v_0 = 0.5$. The characteristic polynomial is $\Upsilon(\xi) = \xi^2 - 0.940789\xi - 0.0592105 + 2.93355\epsilon$. By simultaneously solving $\Upsilon(1) > 0, \Upsilon(-1) > 0$ and $\Upsilon(0) < 1$, it is seen that $0 < \epsilon < 0.361068$. As a result, if $0 < \epsilon < 0.361068$, the fixed point E_2 is LAS. The bifurcation value is calculated to be $\epsilon = 0.361068$, and the interior fixed point of model (1.6) is calculated to be $E_2 = (0.666667, 0.532164)$. $\xi_{1,2} = 0.470395 \pm 0.882456i$ with $|\xi_{1,2}| = 1$ are the eigenvalues of $J(E_2)$. It validates the NS bifurcation of the model (1.6) at E_2 when ϵ reaches 0.361068.

Figure 5a,5b displays the bifurcation diagrams of the model (1.6). MLE graph of model (1.6) is depicted in Figure 5e. The bifurcation diagrams demonstrate that the fixed point E_2, which is stable for $0 < \epsilon < 0.361068$, becomes unstable owing to the emergence of NS bifurcation at $\epsilon = 0.361068$. We analyze the same parameter values and initial values for the controlled model (4.1) with $\rho = 0.9$. If $0 < \epsilon < 0.401186$, the fixed point E_2 is stable for these values. The controlled model's bifurcation diagrams show that the NS bifurcation has been postponed. See Figure 5c,5d. When ϵ crosses over 0.401186, the controlled model undergoes NS bifurcation. By employing small control parameter values of ρ, the NS bifurcation may be postponed over a greater range of ϵ.

5.3. PD bifurcation analysis by varying h

Consider:

$$r = 3.6, k = 0.93, a = 3.5, b = 0.8, d = 0.7, \epsilon = 0.85$$

with the initial conditions $(u_0, v_0) = (0.9, 0.2)$ for the model (1.6). The positive fixed point of (1.6) is $E_2 = (0.875, 0.159073)$. The eigenvalues of $J(E_2)$ for $h \approx 0.777616$ are $\lambda_1 = -1, \lambda_2 = 0.942768$, confirming that the model (1.6) goes through PD bifurcation at E_2 as the bifurcation parameter h crosses 0.777616. See Figure 6a,6c. We consider the same parameter values for the controlled model (4.1) with $\rho = 0.95$. The controlled model's bifurcation diagram reveals that the PD bifurcation has been postponed. See Figure 6b. When h crosses through 0.818543, the controlled model suffers from PD bifurcation. By employing small control parameter values ρ, the PD bifurcation can be postponed over a longer range of h.

Remark 5.1. *To the best of our knowledge, the dynamic behavior of a continuous-time predator-prey model with a square root functional response and slow-fast effect has not been investigated. The equivalent continuous-time predator-prey model* (1.2) *to our model* (1.6) *is investigated in [22]. Their investigation shows that the model* (1.2) *has two boundary fixed points and a positive fixed point. Moreover, it is shown that model* (1.2) *undergoes transcritical and NS bifurcation at the positive fixed point. In this paper, we investigate that model* (1.6) *has two boundary fixed points and a positive fixed. Moreover, we proved that the model* (1.6) *experiences PD and NS bifurcation at the positive fixed point. Our investigation reveals that the discrete model* (1.6) *has richer dynamics than the continuous model* (1.2).

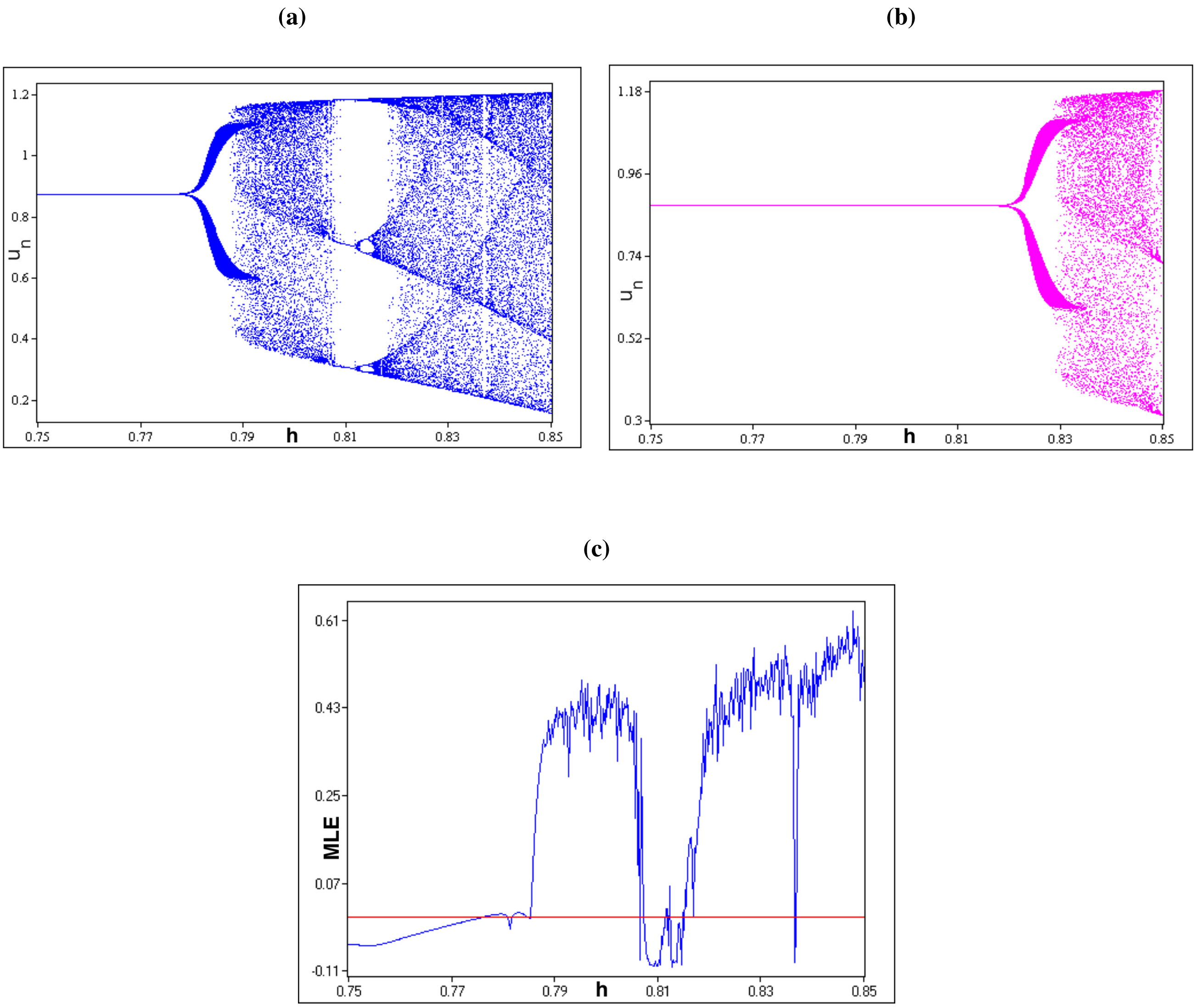

Figure 6. Bifurcation diagram of u_n for model (1.6), (4.1) and MLE graph of (1.6) by taking $\rho = 0.95, r = 3.6, k = 0.93, a = 3.5, b = 0.8, d = 0.7, \epsilon = 0.85, u_0 = 0.9,\ v_0 = 0.2, h \in [0.75, 0.85]$.

6. Conclusions

We present and explore a discrete slow-fast predator-prey model with herd behavior. The model has three fixed points: two boundary fixed points always existing and one interior fixed point that exists only if the prey carrying capacity is large enough. It is determined that the trivial fixed point is unstable. Within the appropriate parameter range, it is found that the boundary fixed point $(\sqrt{k}, 0)$ is stable. If the prey growth rate is sufficiently low and the predator death rate is within a specific interval, then the boundary fixed point $(\sqrt{k}, 0)$ is stable, indicating that the predator population will go to extinction due to a lack of food source. Moreover, the topological classification of the interior fixed point is presented. It is shown that both prey and predator populations experience PD and NS bifurcation around the interior fixed point. Using bifurcation theory and the center manifold theorem, the parametric conditions for the direction and presence of both kinds of bifurcations were derived. The occurrence of both PD bifurcation and NS bifurcation at the positive fixed point indicates that the predator-prey model is undergoing significant changes in its population dynamics under certain parameter conditions. The transitions from stable equilibrium to oscillatory behavior can have profound ecological implications, potentially leading to complex population dynamics, altered ecosystem structure and impacts on the stability of the entire ecological community. Understanding these bifurcations is crucial for predicting and managing the ecological consequences of changes in the predator-prey system. A hybrid control method is used to control the chaotic behavior of model (1.6). Furthermore, some numerical simulations are provided to demonstrate the theoretical results. The chaotic attractor depicted in Figure 2f ensures chaos in the model. Consequently, both forms of bifurcations may be controlled over a maximum control parameter range.

Furthermore, using slow-fast factor ϵ as the bifurcation parameter, it is demonstrated that the model undergoes NS bifurcation at the interior fixed point for larger values of slow-fast factor. Biologically, if the slow-fast factor ϵ is small, the predator's death rate will be much lower than the prey's growth rate. As a result, the predator will have enough food, resulting in the stability of the interior fixed point. This is reasonable because the predator can sustain itself while not growing too large to wipe out the prey due to its slow growth. Furthermore, if the slow-fast factor ϵ is large, the predator's death rate and the prey's growth rate are roughly equal. The slow growth of predators will inevitably lead to the instability of the interior fixed point.

Use of AI tools declaration

The authors declare that they have not used artificial intelligence (AI) tools in the creation of this article.

Acknowledgements

The authors extend their appreciation to the Deputyship for Research & Innovation, Ministry of Education in Saudi Arabia for funding this research through the project number IFP-IMSIU-2023095. The authors also appreciate the Deanship of Scientific Research at Imam Mohammad Ibn Saud Islamic University (IMSIU) for supporting and supervising this project.

Conflict of interest

The authors declare no conflicts of interest.

References

1. E. Aulisa, S. R. J. Jang, Continuous-time predator-prey systems with allee effects in the prey, *Math. Comput. Simul.*, **105** (2014), 1–16. https://doi.org/10.1016/j.matcom.2014.04.004
2. F. Wang, R. Yang, Y. Xie, J. Zhao, Hopf bifurcation in a delayed reaction diffusion predator-prey model with weak allee effect on prey and fear effect on predator, *AIMS Math.*, **8** (2023), 17719–17743. https://doi.org/10.3934/math.2023905
3. S. S. Askar, On complex dynamics of differentiated products: cournot duopoly model under average profit maximization, *Discrete Dyn. Nat. Soc.*, **2022** (2022), 1–14. https://doi.org/10.1155/2022/8677470
4. R. Ahmed, N. Ali, F. M. Rana, Analysis of a cournot-bertrand duoploy game with differentiated products: stability, bifurcation and control, *Asian Res. J. Math.*, **18** (2022), 115–125. https://doi.org/10.9734/arjom/2022/v18i1030422
5. N. A. Shah, A. A. Zafar, S. Akhtar, General solution for MHD-free convection flow over a vertical plate with ramped wall temperature and chemical reaction, *Arab. J. Math.*, **7** (2018), 49–60. https://doi.org/10.1007/s40065-017-0187-z
6. C. Fetecau, N. A. Shah, D. Vieru, General solutions for hydromagnetic free convection flow over an infinite plate with newtonian heating, mass diffusion and chemical reaction, *Commun. Theor. Phys.*, **68** (2017), 768. https://doi.org/10.1088/0253-6102/68/6/768
7. I. Khan, N. A. Shah, L. C. C. Dennis, A scientific report on heat transfer analysis in mixed convection flow of maxwell fluid over an oscillating vertical plate, *Sci. Rep.*, **7** (2017), 40147. https://doi.org/10.1038/srep40147
8. A. J. Lotka, Elements of physical biology, *Science Progress in the Twentieth Century (1919–1933)*, **21** (1926), 341–343.
9. V. Volterra, Fluctuations in the abundance of a species considered mathematically, *Nature*, **118** (1926), 558–560. https://doi.org/10.1038/118558a0
10. H. Freedman, G. Wolkowicz, Predator-prey systems with group defence: the paradox of enrichment revisited, *Bull. Math. Biol.*, **48** (1986), 493–508.
11. C. S. Holling, Some characteristics of simple types of predation and parasitism, *Can. Entomol.*, **91** (1959), 385–398. https://doi.org/10.4039/ent91385-7
12. P. H. Crowley, E. K. Martin, Functional responses and interference within and between year classes of a dragonfly population, *J. N. Am. Benthol. Soc.*, **8** (1989), 211–221. https://doi.org/10.2307/1467324
13. J. R. Beddington, Mutual interference between parasites or predators and its effect on searching efficiency, *J. Anim. Ecol.*, **44** (1975), 331–340. https://doi.org/10.2307/3866

14. D. L. DeAngelis, R. A. Goldstein, R. V. O'Neill, A model for tropic interaction, *Ecology*, **56** (1975), 881–892. https://doi.org/10.2307/1936298
15. H. J. Alsakaji, S. Kundu, F. A. Rihan, Delay differential model of one-predator two-prey system with monod-haldane and holling type ii functional responses, *Appl. Math. Comput.*, **397** (2021), 125919. https://doi.org/10.1016/j.amc.2020.125919
16. C. Arancibia-Ibarra, P. Aguirre, J. Flores, P. van Heijster, Bifurcation analysis of a predator-prey model with predator intraspecific interactions and ratio-dependent functional response, *Appl. Math. Comput.*, **402** (2021), 126152. https://doi.org/10.1016/j.amc.2021.126152
17. X. Chen, X. Zhang, Dynamics of the predator-prey model with the sigmoid functional response, *Stud. Appl. Math.*, **147** (2021), 300–318. https://doi.org/10.1111/sapm.12382
18. M. F. Elettreby, A. Khawagi, T. Nabil, Dynamics of a discrete prey-predator model with mixed functional response, *Int. J. Bifurcat. Chaos*, **29** (2019), 1950199. https://doi.org/10.1142/s0218127419501992
19. P. Panja, Combine effects of square root functional response and prey refuge on predator-prey dynamics, *Int. J. Model. Simul.*, **41** (2021), 426–433. https://doi.org/10.1080/02286203.2020.1772615
20. S. M. Sohel Rana, U. Kulsum, Bifurcation analysis and chaos control in a discrete-time predator-prey system of leslie type with simplified holling type iv functional response, *Discrete Dyn. Nat. Soc.*, **2017** (2017), 9705985. https://doi.org/10.1155/2017/9705985
21. X. Han, C. Lei, Bifurcation and turing instability analysis for a space- and time-discrete predator-prey system with smith growth function, *Chaos, Solitons Fract.*, **166** (2023), 112910. https://doi.org/10.1016/j.chaos.2022.112910
22. V. Ajraldi, M. Pittavino, E. Venturino, Modeling herd behavior in population systems, *Nonlinear Anal.: Real World Appl.*, **12** (2011), 2319–2338. https://doi.org/10.1016/j.nonrwa.2011.02.002
23. P. A. Braza, Predator-prey dynamics with square root functional responses, *Nonlinear Anal.: Real World Appl.*, **13** (2012), 1837–1843. https://doi.org/10.1016/j.nonrwa.2011.12.014
24. M. G. Mortuja, M. K. Chaube, S. Kumar, Dynamic analysis of a predator-prey system with nonlinear prey harvesting and square root functional response, *Chaos, Solitons Fract.*, **148** (2021), 111071. https://doi.org/10.1016/j.chaos.2021.111071
25. D. Pal, P. Santra, G. S. Mahapatra, Predator-prey dynamical behavior and stability analysis with square root functional response, *Int. J. Appl. Comput. Math.*, **3** (2017), 1833–1845. https://doi.org/10.1007/s40819-016-0200-9
26. S. M. Salman, A. M. Yousef, A. A. Elsadany, Stability, bifurcation analysis and chaos control of a discrete predator-prey system with square root functional response, *Chaos, Solitons Fract.*, **93** (2016), 20–31. https://doi.org/10.1016/j.chaos.2016.09.020
27. N. C. Stenseth, W. Falck, O. N. Bjornstad, C. J. Krebs, Population regulation in snowshoe hare and canadian lynx: Asymmetric food web configurations between hareandlynx, *Proceedings of the National Academy of Sciences*, **94** (1997), 5147–5152. https://doi.org/10.1073/pnas.94.10.5147
28. G. Hek, Geometric singular perturbation theory in biological practice, *J. Math. Biol.*, **60** (2010), 347–386. https://doi.org/10.1007/s00285-009-0266-7

29. S. Rinaldi, S. Muratori, Slow-fast limit cycles in predator-prey models, *Ecol. Model.*, **61** (1992), 287–308. https://doi.org/10.1016/0304-3800(92)90023-8

30. W. Liu, D. Cai, Bifurcation, chaos analysis and control in a discrete-time predator-prey system, *Adv. Differ. Equ.*, **2019** (2019), 11. https://doi.org/10.1186/s13662-019-1950-6

31. A. Q. Khan, I. Ahmad, H. S. Alayachi, M. S. M. Noorani, A. Khaliq, Discrete-time predator-prey model with flip bifurcation and chaos control, *Math. Biosci. Eng.*, **17** (2020), 5944–5960. https://doi.org/10.3934/mbe.2020317

32. Z. AlSharawi, S. Pal, N. Pal, J. Chattopadhyay, A discrete-time model with non-monotonic functional response and strong allee effect in prey, *J. Differ. Equ. Appl.*, **26** (2020), 404–431. https://doi.org/10.1080/10236198.2020.1739276

33. R. Ahmed, A. Ahmad, N. Ali, Stability analysis and neimark-sacker bifurcation of a nonstandard finite difference scheme for lotka-volterra prey-predator model, *Commun. Math. Biol. Neurosci.*, **2022** (2022), 61. https://doi.org/10.28919/cmbn/7534

34. P. A. Naik, Z. Eskandari, M. Yavuz, J. Zu, Complex dynamics of a discrete-time Bazykin-Berezovskaya prey-predator model with a strong Allee effect, *J. Comput. Appl. Math.*, **413** (2022), 114401. https://doi.org/10.1016/j.cam.2022.114401

35. S. M. Sohel Rana, Dynamics and chaos control in a discrete-time ratio-dependent holling-tanner model, *J. Egypt. Math. Soc.*, **27** (2019), 48. https://doi.org/10.1186/s42787-019-0055-4

36. P. Baydemir, H. Merdan, E. Karaoglu, G. Sucu, Complex dynamics of a discrete-time prey-predator system with leslie type: stability, bifurcation analyses and chaos, *Int. J. Bifurcat. Chaos*, **30** (2020), 2050149. https://doi.org/10.1142/s0218127420501497

37. M. Zhao, C. Li, J. Wang, Complex dynamic behaviors of a discrete-time predator-prey system, *J. Appl. Anal. Comput.*, **7** (2017), 478–500. https://doi.org/10.11948/2017030

38. A. A. Khabyah, R. Ahmed, M. S. Akram, S. Akhtar, Stability, bifurcation, and chaos control in a discrete predator-prey model with strong allee effect, *AIMS Math..*, **8** (2023), 8060–8081. https://doi.org/10.3934/math.2023408

39. S. Akhtar, R. Ahmed, M. Batool, N. A. Shah, J. D. Chung, Stability, bifurcation and chaos control of a discretized leslie prey-predator model, *Chaos, Solitons Fract.*, **152** (2021), 111345. https://doi.org/10.1016/j.chaos.2021.111345

40. A. Tassaddiq, M. S. Shabbir, Q. Din, H. Naaz, Discretization, bifurcation, and control for a class of predator-prey interactions, *Fractal Fract.*, **6** (2022), 31. https://doi.org/10.3390/fractalfract6010031

41. Z. Zhu, Y. Chen, Z. Li, F. Chen, Stability and bifurcation in a Leslie-Gower predator-prey model with allee effect, *Int. J. Bifurcat. Chaos*, **32** (2022), 2250040. https://doi.org/10.1142/s0218127422500407

42. C. Lei, X. Han, W. Wang, Bifurcation analysis and chaos control of a discrete-time prey-predator model with fear factor, *Math. Biosci. Eng.*, **19** (2022), 6659–6679. https://doi.org/10.3934/mbe.2022313

43. X. Han, C. Lei, Stability, bifurcation analysis and pattern formation for a nonlinear discrete predator-prey system, *Chaos, Solitons Fract.*, **173** (2023), 113710. https://doi.org/10.1016/j.chaos.2023.113710

44. A. C. J. Luo, *Regularity and complexity in dynamical systems*, Springer, 2012. https://doi.org/10.1007/978-1-4614-1524-4

45. S. Wiggins, *Introduction to applied nonlinear dynamical systems and chaos*, Springer, 2003. https://doi.org/10.1007/b97481

46. J. Guckenheimer, P. Holmes, *Nonlinear oscillations, dynamical systems, and bifurcations of vector fields*, Springer, 1983. https://doi.org/10.1007/978-1-4612-1140-2

47. R. Ahmed, M. S. Yazdani, Complex dynamics of a discrete-time model with prey refuge and holling type-ii functional response, *J. Math. Comput. Sci.*, **12** (2022), 113. https://doi.org/10.28919/jmcs/7205

48. X. S. Luo, G. Chen, B. H. Wang, J. Q. Fang, Hybrid control of period-doubling bifurcation and chaos in discrete nonlinear dynamical systems, *Chaos, Solitons Fract.*, **18** (2003), 775–783. https://doi.org/10.1016/s0960-0779(03)00028-6